

High performance infrared detectors compatible with CMOS-circuit process

Chao Wang(王超), Ning Li(李宁), Ning Dai(戴宁), Wang-Zhou Shi(石旺舟), Gu-Jin Hu(胡古今), He Zhu(朱贺)
Citation: Chin. Phys. B, 2021, 30 (**5**): 050702. DOI: 10.1088/1674-1056/abd6fb
Journal homepage: http://cpb.iphy.ac.cn; http://iopscience.iop.org/cpb

What follows is a list of articles you may be interested in

Investigation of copper sulfate pentahydrate dehydration by terahertz time-domain spectroscopy

Yuan-Yuan Ma(马媛媛), Hao-Chong Huang(黄昊翀), Si-Bo Hao(郝思博), Wei-Chong Tang(汤伟冲), Zhi-Yuan Zheng(郑志远), Zi-Li Zhang(张自力)
Chin. Phys. B, 2019, 28 (**6**): 060702. DOI: 10.1088/1674-1056/28/6/060702

4.3 THz quantum-well photodetectors with high detection sensitivity

Zhenzhen Zhang(张真真), Zhanglong Fu(符张龙), Xuguang Guo(郭旭光), Juncheng Cao(曹俊诚)
Chin. Phys. B, 2018, 27 (**3**): 030701. DOI: 10.1088/1674-1056/27/3/030701

Experimental research on spectrum and imaging of continuous-wave terahertz radiation based on interferometry

Tie-Lin Lu(卢铁林), Hui Yuan(袁 慧), Ling-Qin Kong(孔令琴), Yue-Jin Zhao(赵跃进), Liang-Liang Zhang(张亮亮), Cun-Lin Zhang(张存林)
Chin. Phys. B, 2016, 25 (**8**): 080702. DOI: 10.1088/1674-1056/25/8/080702

Spectroscopic measurements and terahertz imaging of the cornea using a rapid scanning terahertz time domain spectrometer

Wen-Quan Liu(刘文权), Yuan-Fu Lu(鲁远甫), Guo-Hua Jiao(焦国华), Xian-Feng Chen(陈险峰), Zhi-Sheng Zhou(周志盛), Rong-Bin She(佘荣斌), Jin-Ying Li(李金瑛), Si-Hai Chen(陈四海), Yu-Ming Dong (董玉明), Jian-Cheng Lü(吕建成)
Chin. Phys. B, 2016, 25 (**6**): 060702. DOI: 10.1088/1674-1056/25/6/060702

Theoretical models for designing a 220-GHz folded waveguide backward wave oscillator

Cai Jin-Chi, Hu Lin-Lin, Ma Guo-Wu, Chen Hong-Bin, Jin Xiao, Chen Huai-Bi
Chin. Phys. B, 2015, 24 (**6**): 060701. DOI: 10.1088/1674-1056/24/6/060701

High performance infrared detectors compatible with CMOS-circuit process*

Chao Wang(王超)[1,2], Ning Li(李宁)[1], Ning Dai(戴宁)[1,3,4,†], Wang-Zhou Shi(石旺舟)[5], Gu-Jin Hu(胡古今)[5,‡], and He Zhu(朱贺)[6]

[1] *State Key Laboratory of Infrared Physics, Shanghai Institute of Technical Physics, Chinese Academy of Sciences, Shanghai* 200083, *China*
[2] *University of Chinese Academy of Sciences, Beijing* 100049, *China*
[3] *College of Physics and Optoelectronic Engineering, Hangzhou Institute for Advanced Study, University of Chinese Academy of Sciences, Hangzhou* 310024, *China*
[4] *Jiangsu Collaborative Innovation Center of Photovolatic Science and Engineering, Changzhou* 213164, *China*
[5] *Department of Physics, College of Mathematics and Science, Shanghai Normal University, Shanghai* 200234, *China*
[6] *Hangzhou Dianzi University, Hangzhou* 310018, *China*

(Received 10 August 2020; revised manuscript received 18 December 2020; accepted manuscript online 28 December 2020)

A type of Si-based blocked impurity band photoelectric detector with a planar architecture is designed and demonstrated by a modified silicon semiconductor processing technique. In this route, multiple ion implantation is utilized to ensure the uniform distribution of the P elements in silicon, and rapid thermal annealing treatment is used to activate the P atoms and reduce damages caused by ion-implantation. The fabricated prototype device exhibits an excellent photoelectric response performance. With a direct current (DC) bias voltage of −2.3 V, the device detectivity to blackbody irradiation is as high as 5×10^{13}cm·Hz$^{1/2}$/W, which corresponds to a device responsivity of nearly 4.6 A/W, showing their potential applications in infrared detection, infrared astrophysics, and extraterrestrial life science. In particular, the developed device preparation process is compatible with that for the CMOS-circuit, which greatly reduces the manufacturing cost.

Keywords: Si:P, long wavelength detectors, blocked impurity band, terahertz

PACS: 07.57.Kp, 33.20.Ea, 85.60.Gz **DOI:** 10.1088/1674-1056/abd6fb

1. Introduction

Electromagnetic waves in a wavelength range of ∼ 1 μm–300 μm are widely used in infrared imaging, security inspection, earth observation, infrared astrophysics, extraterrestrial life science, and other fields.[1–5] A variety of detection technologies have been developed in order to meet various demands.[6–8] Generally speaking, infrared and terahertz detectors working in this frequency range can be divided into photoelectric devices and thermoelectric devices according to their working principles.[9]

The response speeds of the photoelectric devices are very fast, specifically, in a nanosecond range, while those of the thermoelectric devices are very slow, in a millisecond range. In the processing technology, photoelectric-based detectors are relatively complex due to the requirements for special materials and device structures.

Recent years, the so-called photoconductive blocked impurity band (BIB) infrared detectors have attracted much attention again due to their outstanding merits such as low dark currents, large photoconductivity gains, high resistance to irradiation, *etc*.[10–13] Petroff and Michael first proposed and demonstrated this type of device and established the basic model of responsivity and noise of the BIB detector.[14] For the silicon-based BIB device, the photoelectric response wavelength is mainly determined by the ionization energy of the doped atoms in the active layer. By introducing different impurities, peak wavelength can be tuned from 2.3 μm to 31 μm.[10,11,13] Most of the existing silicon-based BIB photoelectric detectors are fabricated by molecular beam epitaxy and standard Si process, which are expensive in cost.[5,10,11,13,15–20] Ion-implantation is a relatively-simple, highly-efficient, and cheap semiconductor-processing technology. It was first used to fabricate BIB detectors by Beeman *et al.* in 2007.[21] Illuminated by their ideas, we investigate a kind of planar configuration of Si-based photoconductive BIB detectors that are fabricated by using a modified Si-based process. With a DC bias voltage of −2.3 V the normalized peak detectivity (D^*) is as high as 4.9×10^{13} cm·Hz$^{1/2}$/W, and the responsivity is nearly 4.58 A/W. Both parameters are comparable to or even superior to the corresponding results reported in the literature.[5,10–12,16,19,21] Very importantly, the manufacturing method used for the present Si:P BIB detectors is almost compatible with that for the CMOS-circuit, thus significantly reducing the fabrication cost.

*Project supported by the National Natural Science Foundation of China (Grant Nos. 11933006, 61805060, and 61290304).
†Corresponding author. E-mail: ndai@mail.sitp.ac.cn
‡Corresponding author. E-mail: hugj@shnu.edu.cn
© 2021 Chinese Physical Society and IOP Publishing Ltd

2. Experimental procedure

The device structure used here is similar to that described in Refs. [10–12,16]. Figure 1 shows the schematic diagram of device structure and the process flow chart of a Si:P photoconductive BIB detector. As shown in Fig. 1, the detector consists of two Al contact regions, a P-doped Si absorbing layer, an intrinsic Si blocking layer, and a passivation layer. The high-purity Si wafer, grown by the floating zone method, has a resistivity of 10^4 Ω·cm. The two contact regions, respectively, with a P-atom density of 10^{20} cm^{-3} and 5×10^{17} cm^{-3} were achieved by P-ion implantation. In the direction of photocurrent transport, the widths of blocking layer and absorbing layer are 3 μm and 50 μm, respectively. The area of the photosensitive region is 50 μm×1000 μm. To ensure the uniform distribution of the P elements, multiple ion implantations were performed. The rapid thermal annealing at 950 °C for 90 s was implemented to activate the P atoms and reduce the damage caused by ion-implantation. A layer of SiN_x passivating film with a thickness of 200 nm was deposited on a Si wafer surface by plasma-enhanced chemical vapor deposition. Owing to its compactness better than that of SiO_2, SiN_x is more effective for the passivation of Si surface. In addition, SiN_x shows better performance in preventing atmospheric moisture from permeating into the device. Finally, a 600-nm-thick Al layer was prepared by using the electron beam evaporation, followed by reactive ion etching and lithographic patterning. A 30-min annealing treatment at 450 °C was conducted for the deposited Al films to form Ohmic contact with the heavily-doped Si matrices.

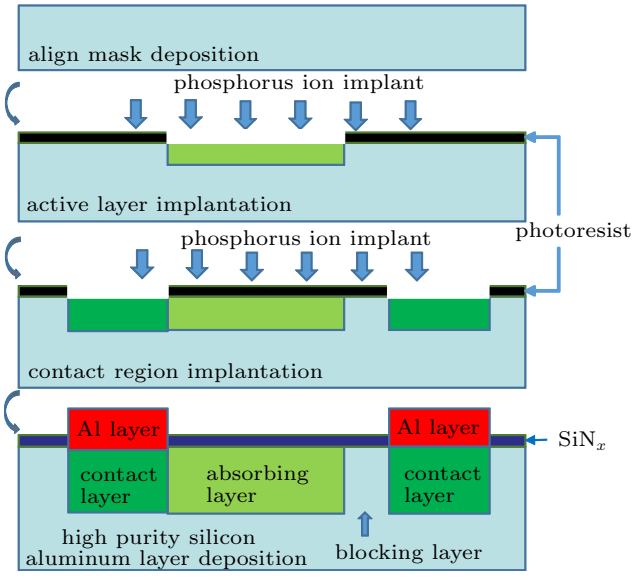


Fig. 1. Schematic diagram of device structure and process flow chart of BIB detector.

The packaged detectors were mounted into a closed cycle cryogenic dewar equipped with a temperature controller. The photocurrent spectra were measured by a Nicolet 6700 Fourier transform infrared spectrometer, and the current–voltage (I–V) characteristic curves were recorded via a Kethily 236 semiconductor parameter analyzer. The blackbody response measurement system includes an 800-K blackbody source, a low-noise current amplifier (Stanford Research SR570), and a lock-in amplifier (Stanford Research SR830). The blackbody signal was chopped at a frequency of 277 Hz. Unless otherwise stated, all the photoelectric response measurements were performed at 5 K, and the infrared radiation was along the surface normal to the Si wafer.

3. Results and discussion

In a photoconductive BIB detector, the absorbing layer absorbs photons with very low energy, generating electron hole pairs. The electrons and holes are separated by using an applied voltage to drive photocurrent. The blocking layer is used to block the dark current. The performance of a BIB detector is mainly limited by its dark current (leakage current). The lower the leakage current, the higher the device detectivity is. Figure 2 displays the typical I–V characteristic curves of an ion-implanted Si:P BIB detector at several temperatures. It can be seen that the leakage current increases with temperature increasing. The reason is that with temperature increasing, more impurity states with shallow energy levels in Si material are thermally excited and release more electrons to conductive band, giving rise to a larger dark current at the same DC bias voltage. At 5 K, the I–V curve of the Si:P BIB detector shows a steep on-off character and the dark current is less than 0.05 nA in a bias voltage range from −2.3 V to 2.3 V, revealing an important role of the blocking layer in inhibiting dark current. The breakdown voltage of the detector is about ±2.4 V. Since a P atom has five valance electrons and acts as a donor in Si, the fabricated Si:P BIB detectors are all of n-type. For a BIB detector, the background impurity concentration N_d in the blocking layer is an important parameter determining the width of the depletion region and the tunneling current. Generally, the resistivity of the epitaxial Si blocking layer is about 10 Ω·cm, corresponding to a doping concentration of 10^{14} atom/cm^3.[17] However, here in this work, the resistivity of the FZ-Si blocking layer reaches 20000 Ω·cm at room temperature, N_d in the blocking layer is $\sim 10^{12}$ cm^{-3} much lower than that in the epitaxial Si blocking layer and activating Si layer, resulting in a wider depletion region. On the other hand, in the blocking layer the average distance between two adjacent donor impurities is larger than 50 nm, the ionized $^+$P cannot move freely and the impurity bands are interrupted. Thus, the detector leakage current is effectively reduced by the blocking layer. Additionally, according to semiconductor physics, a PN junction is termed electrical breakdown when the leakage current abruptly increase to one thousand times of its initial current value at a given reverse bias voltage. This

voltage is called breakdown voltage. The breakdown mechanism of a PN junction generally includes avalanche breakdown, Zener breakdown, and thermal breakdown. Because the thickness of the blocking layer is about 3 μm, the width of the potential barrier in the depletion region is on the order of micrometer. Herein the breakdown of the Si:P BIB detector should be triggered by the avalanche breakdown.

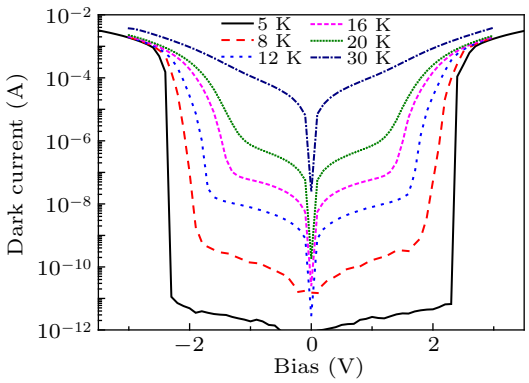


Fig. 2. Typical *I*–*V* characteristic curves of ion-implanted Si:P BIB detector at various temperatures.

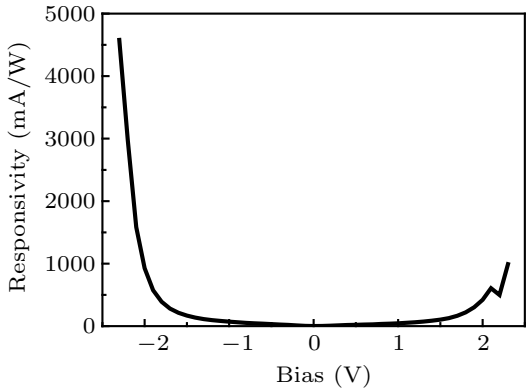


Fig. 3. Variation of detector responsivity with bias voltage at 5 K.

Figure 3 shows the responsivity for one of our Si:P BIB devices. The detector responsivity is measured by an 800-K blackbody source chopped at a frequency of 277 Hz. It can be found that the response photocurrent of the device increases slowly with the bias decreasing from 2.0 V to −2.0 V. When the DC bias changes gradually from 2.0 V to the threshold voltage of −2.4 V, the responsivity increases quickly and reaches a value of 4.58 A/W at −2.3 V. At 5 K, the dark current of the detector is on the order of pA in a range of −2.0 V to −2.3 V, so that the measured blackbody responsivity is dominantly contributed by photocurrent, indicating that the fabricated device has a very high photoelectric conversion efficiency.

The D^* is an essential physical quantity characterizing the performance of a photoelectric detector, and expressed as[22]

$$D^* = (R/\sqrt{2qI_{\rm dark}\Delta f})\sqrt{A_{\rm d}\Delta f}, \tag{1}$$

where R is the responsivity, $I_{\rm dark}$ is the dark current, $A_{\rm d}$ is the area of the photosensitive element, q is the electron charge, and Δf is the frequency band width of the current amplifier.

Figure 4 shows the calculated D^* as a function of DC bias voltage for the Si:P BIB detector. The obtained D^* value is as high as 4.9×10^{13} cm·Hz$^{1/2}$/W at a bias voltage of −2.3 V, higher than those reported in Refs. [12,13,16,19]. We believe that both a small leakage current ∼ 0.01 nA and a large responsivity ∼ 4.58 A/W at 5 K and −2.3 V bias are responsible for the high detectivity D^*. For comparing, Table 1 lists the performance parameters of several kinds of BIB detectors.

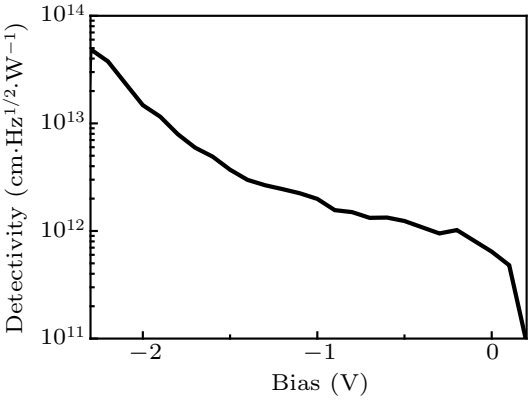


Fig. 4. Detectivity D^* *versus* DC bias voltage of Si:P BIB detector at 5 K.

Table 1. Performance parameters of BIB detectors made by different methods.

BIB detectors	Responsivity (mA/W)	Detectivity (Hz$^{1/2}$/W)	D^* (cm·Hz$^{1/2}$/W)	Specification
Epitaxial Si:As, Ref. [5]	13		6.7×10^{12}	
Ion-implanted Ge:S, Ref. [10]	400		9.7×10^{10}	$T=4$ K, $\lambda_{\rm p}\approx6$ μm
Ion-implanted Ge:B, Ref. [21]	120	1.9×10^{14}		$T=6$ K, $\lambda_{\rm p}\approx90$ μm
Epitaxial Si:As, Ref. [22]	2×10^{3}		10^{13}	
Ion-implanted Si:P, Ref. [23]	4.0×10^{3}		5×10^{12}	$T=4$ K
Ion-implanted Si:P, present work	4.6×10^{3}	2.4×10^{15}	5×10^{13}	$T=5$ K, $T_{\rm blackbody}=800$ K, $\lambda_{\rm p}=27.3$ μm

In order to analyze the energy state of P impurities in the devices, photocurrent response in a mid-infrared-to-far-infrared range were measured by using the Nicolet 6700 Fourier transform infrared spectrometer with a solid substrate beam splitter and internal globar illumination. Figure 5 shows photocurrent response as a function of wavelength of the Si:P BIB detector biased at −1 V. The response wavelength range of the device covers 2.5 μm–35 μm. The abrupt photocurrent decrease at ∼ 16 μm is due to the absorption of the transverse optical phonons and transverse acoustic phonons in silicon,

while the response peat at ∼ 31 μm originates from the transition of P atoms from 1S state to 2P state.[19]

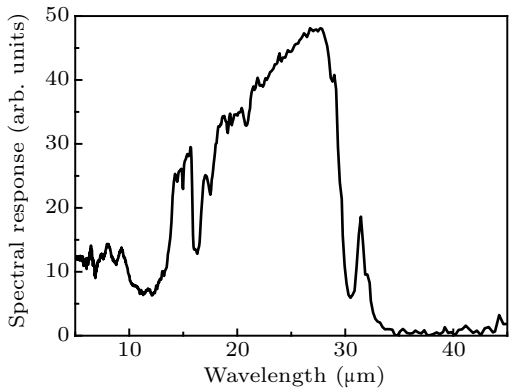


Fig. 5. Spectral response *versus* wavelength of Si:P BIB detector biased at −1 V at 5 K.

The wavelength at the maximum photocurrent response, the peak responsivity, the full width at half maximum of the peak, and the cutoff wavelength toward the long-wavelength are ∼ 27.3 μm, 80.1 A/W, 17.6 μm, and 29.5 μm, respectively. The photocurrent response of the Si:P BIB detectors in the wavelength range of 2.5 μm–35 μm stems from the P atom electron transition caused by the irradiation excitation.[19,23]

4. Summary

In summary, based on multiple ion-implantation and rapid thermal annealing treatment, a modified process is developed to fabricate high performance Si-based blocked impurity band detectors, and a significant reduction in production cost is realized due to a high compatibility of this process technology with CMOS-circuit. Compared with previously reported detectors, the fabricated photoconductive devices display comparable or even better to photoelectric response characteristics. At 5 K and a DC bias voltage of −2.3 V, the responsivity and the detectivity of our best detector to the 800-K blackbody radiation are over 4.0 A/W and 4.5×10^{13} cm·Hz$^{1/2}$/W, which bring light to their potential applications of infrared astrophysics, infrared detection, and extraterrestrial life science.

References

[1] Mcintosh A I, Yang B, Goldup S M, Watkinson M and Donnan R S 2012 *Chem. Soc. Rev.* **41** 2072

[2] Kulesa C 2011 *IEEE Trans. Terahertz Sci. Technol.* **1** 232

[3] Jansen C, Wietzke S, Peters O, Scheller M and Koch M 2010 *Appl. Opt.* **49** 48

[4] Hogue H H, Mlynczak M G, Abedin M N, Masterjohn S A and Huffman J E 2008 *Proc. SPIE -Int. Soc. Opt. Eng.* **7082** 70820E

[5] Stetson S B, Reynolds D B, Stapelbroek M G and Stermer R L 1986 *Proc. SPIE- Int. Soc. Opt. Eng.* **686** 48

[6] James B, Matin A, Joy C, Chen Y Z, Ho A G, Valerio A, Raj S V, Gao Y, Crozier K B and Yu-Lun C 2018 *Nat. Photon.* **12** 601

[7] Wang L, Liu C L, Chen X S, Zhou J, Hu W D, Wang X F, Li J H, Tang W W, Yu A Q and Wang S W 2017 *Adv. Funct. Mater.* **27** 1604414

[8] Huo N, Gupta S and Konstantatos G 2017 *Adv. Mater.* **29** 1606576

[9] Cai X H, Sushkov A B, Suess R J, Jadidi M M, Jenkins G S, Nyakiti L O, Myersward R L, Li S S, Yan J and Gaskill D K 2014 *Nat. Nanotechnol.* **9** 814

[10] Zhu J Q, Zhu H, Xu H L, Weng Z P and Wu H Z 2018 *Infrared Physics & Technology* **92** 13

[11] Hanaoka M, Kaneda H, Oyabu S, Yamagishi M, Hattori Y, Ukai S, Shichi K, Wada T, Suzuki T and Watanabe K 2016 *J. Low Temperature Phys.* **184** 225

[12] Zhu H, Weng Z P, Zhu J Q, *et al.* 2017 *Appl. Phys. Lett.* **111** 053505

[13] Zhu H, Weng Z P, Zhu J Q, Wu H Z, Li N and Dai N 2017 *IEEE Trans. Electron Dev.* **64** 1094

[14] Petroff M D and Michael M G (U.S. Patent) 4568 960 [1986-02-04]

[15] Love P J 2004 *Proc. SPIE -Int. Soc. Opt. Eng.* **5499** 86

[16] Hogue H H, Dereniak E L, Hartke J P, Atkins E, Reynolds D, Levan P D, Sood A K, Salcido M, Dawson L and Longshore R E 2010 *Proc. SPIE* 7780*, Detectors and Imaging Devices: Infrared, Focal Plane, Single Photon*, September 2, 2010, San Diego, California, USA, 778004

[17] Hogue H H, Longshore R E, Sood A K, Mattson R B, Stapelbroek M G, Dereniak E L, Hartke J P, Masterjohn S A, Larsen M F and Elwell J D 2007 *Proc. SPIE* 6660*, Infrared Systems and Photoelectronic Technology II*, September 19, 2007, San Diego, California, USA, 66600S

[18] Liao K S, Li Z F, Wang C, Li L, Zhou X H, Li N and Dai N 2016 *J. Infrared Millim. Waves* **35** 37 (in Chinese)

[19] Liao K S, Li N, Wang C, Li L, Jing Y L, Wen J, Li M Y, Wang H, Zhou X H, Li Z F and Lu W 2014 *Appl. Phys. Lett.* **105** 183903

[20] Liao K S, Li Z F, Li L, Wang C, Zhou X H, Dai N and Li N 2015 *Acta Phys. Sin.* **64** 227302 (in Chinese)

[21] Beeman J W, Goyal S, Reichertz L A and Haller E E 2007 *Infrared Physics & Technology* **51** 60

[22] Szmulowicz F and Madarasz F L 1987 *J. Appl. Phys.* **62** 2533

[23] Zhu H, Wang C, Wang P, He J L and Hu W D 2019 *IEEE Trans. Electron Dev.* **66** 3891